Supporting information

Structural characterization of *H. pylori* dethiobiotin synthetase reveals differences between family members

Przemyslaw J. Porebski, Maria Klimecka, Maksymilian Chruszcz, Robert A. Nicholls, Krzysztof Murzyn, Marianne E. Cuff, Xiaohui Xu, Marcin Cymborowski, Garib N. Murshudov, Alexei Savchenko, Aled Edwards, and Wladek Minor

Figure S1

(A) Schematic representation of the four final reactions of the biotin synthesis pathway

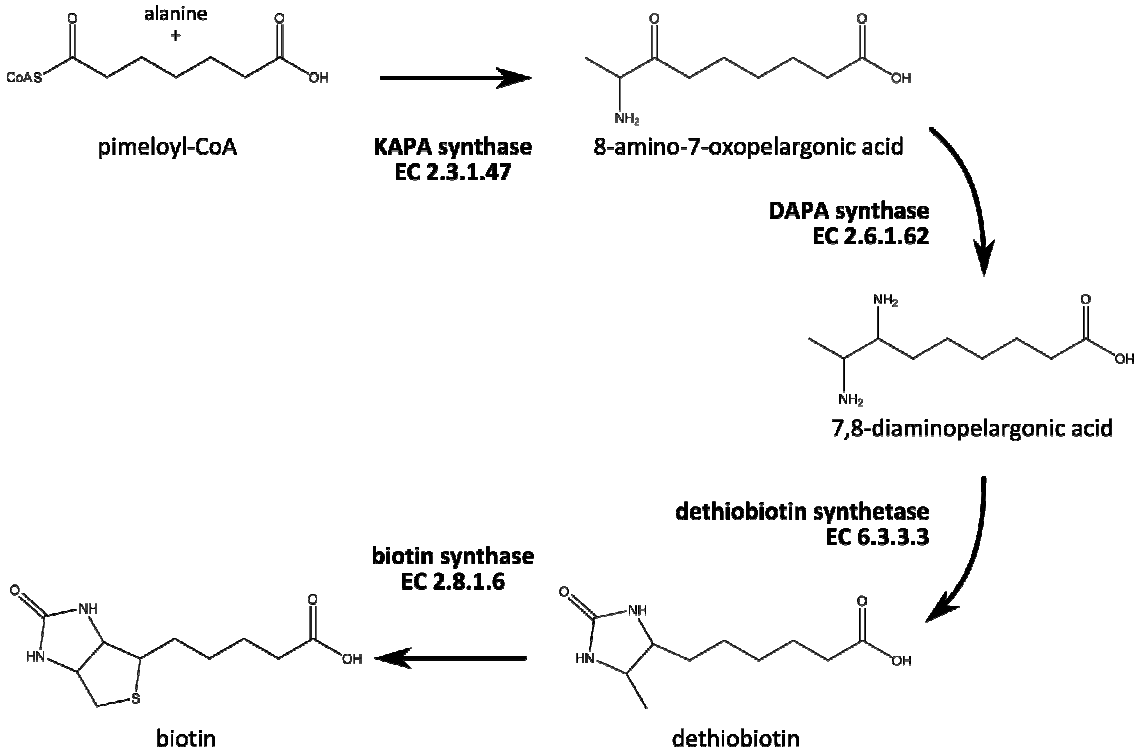

(B) Schematic representation of the reaction catalyzed by the dethiobiotin synthetase.

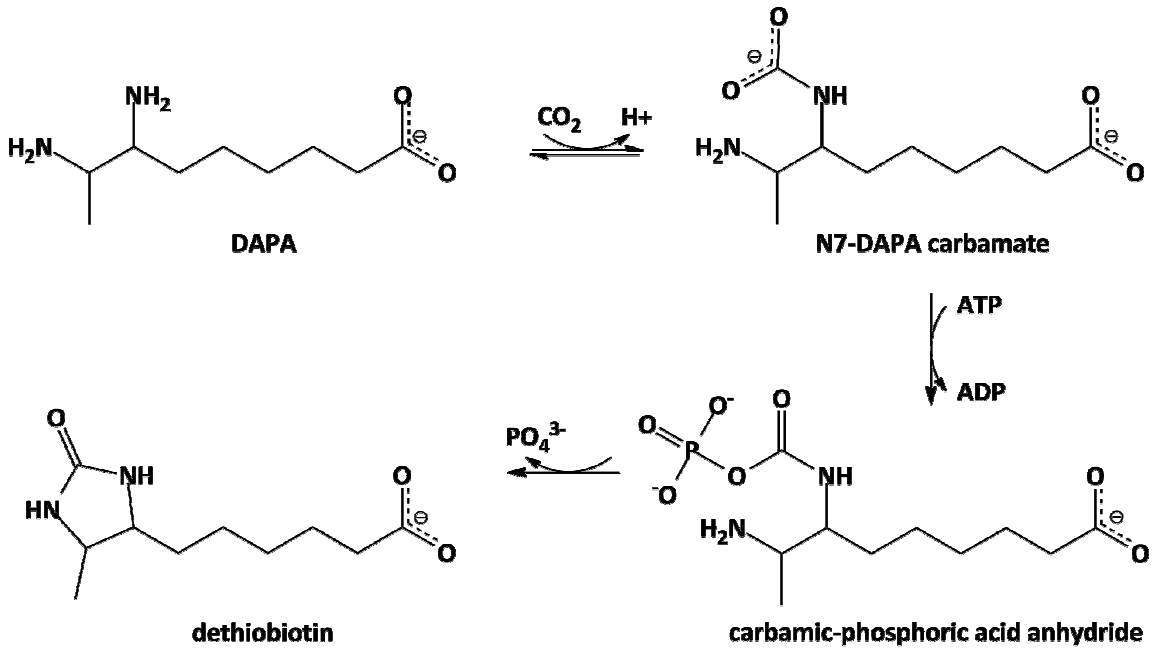

Figure S2

Surfaces of hpDTBS (A) and ecDTBS (B) with residues colored according to function.

Residues forming hydrogen bonds with the polyphosphate moiety of nucleotide are in orange; the residues binding DAPA are in blue (those forming H-bonds in dark blue and those forming the hydrophobic pocket in pale blue); and the residues binding the adenine moiety are in green (those forming H-bonds in dark green and those forming hydrophobic interactions in pale green).

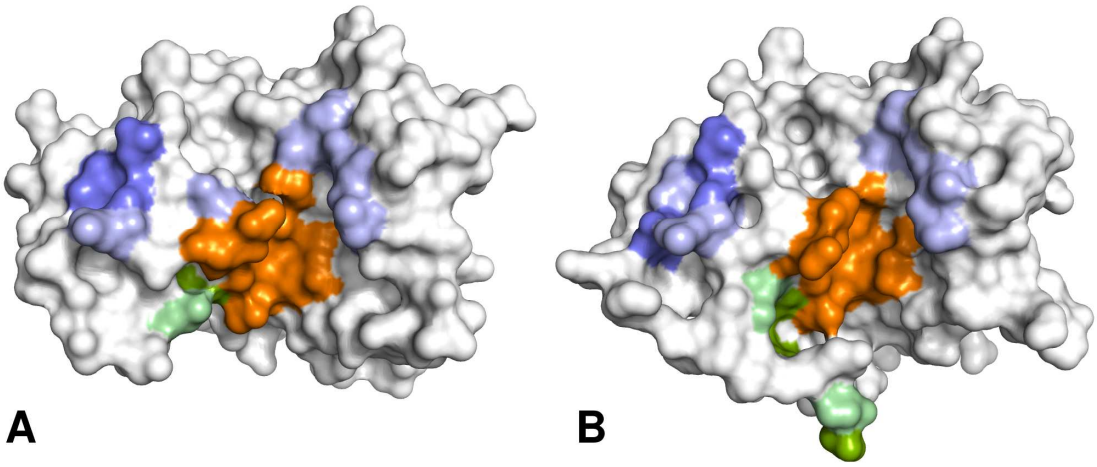

Figure S3

(A) 2-D diagram of DAPA and (B) 8-aminocaprylic acid.

Carbon 7 of DAPA and its associated amino group, which is carbamylated during formation of the ureido ring, is highlighted with a grey box. The lack of the amino group in this position of 8-aminocaprylic acid renders it a nonreactive analog.

(C) Wall-eye stereo view of F_O-F_C omit maps showing ligand density for 8-aminocaprylic acid. The omit map corresponding to ordered 8-aminocaprylic acid from the 3QXH deposit is in green. The omit map corresponding to the disordered 8-aminocaprylic acid from the 3QXC deposit are in blue. Both maps are displayed at the 3σ level.

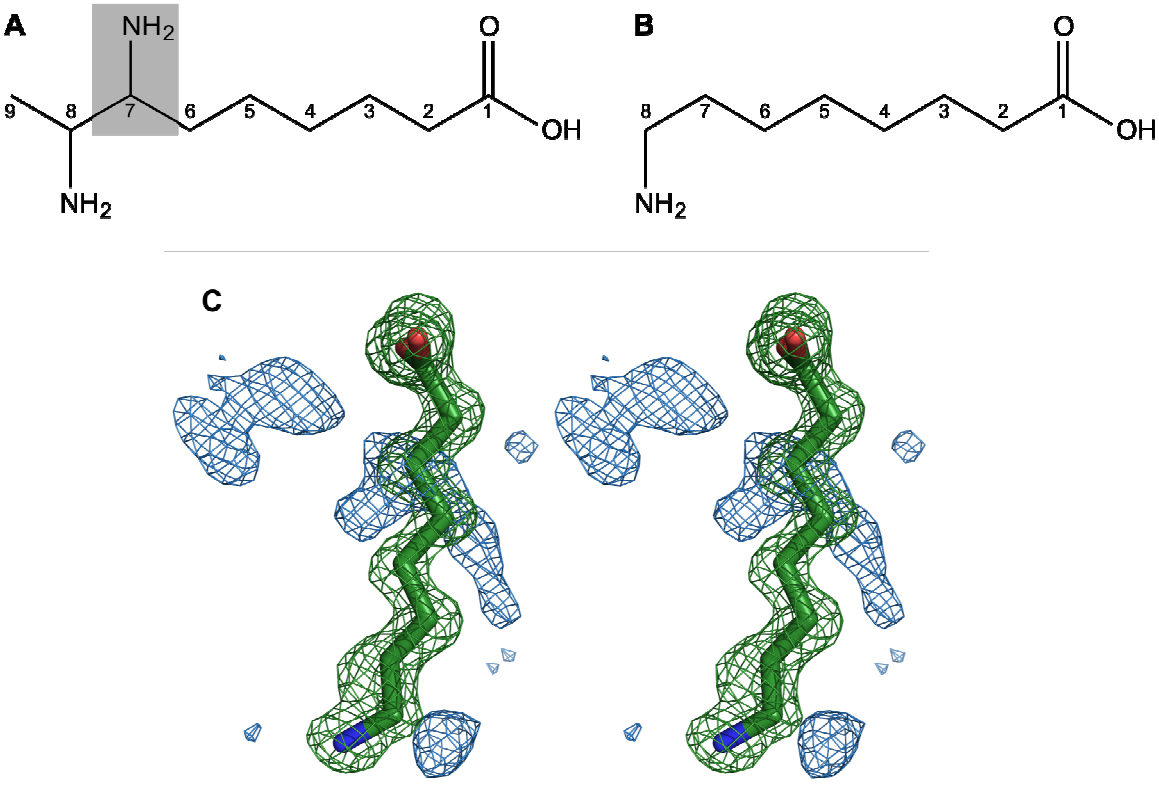

Figure S4

Isothermal titration calorimetry results.

A – ATP binding; **B** – ADP binding

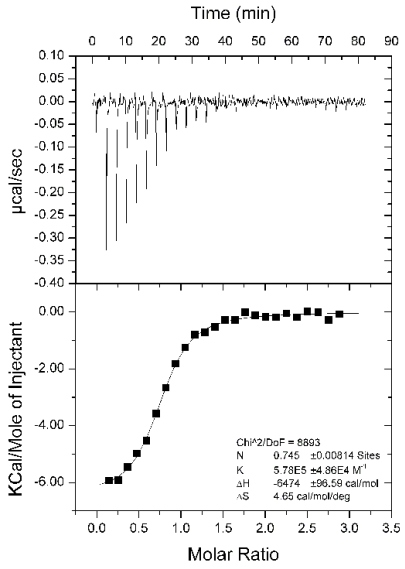

A

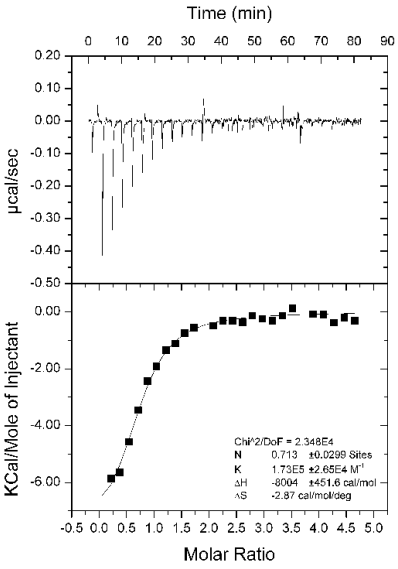

B

Figure S5

F_O-F_C omit maps showing ligand densities for analyzed ligands.

Modeled ligands are represented in black sticks with corresponding electron density maps displayed at the 3σ level in green. PDB code and corresponding complex name are shown below each structure.

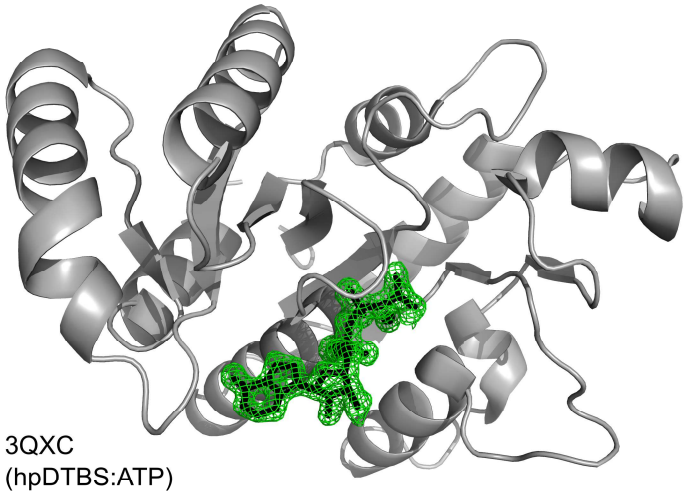

3QXC
(hpDTBS:ATP)

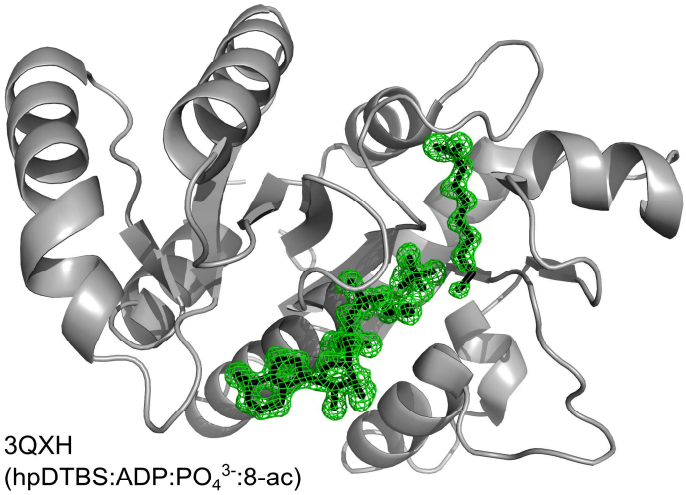

3QXH
(hpDTBS:ADP:PO_4^{3-}:8-ac)

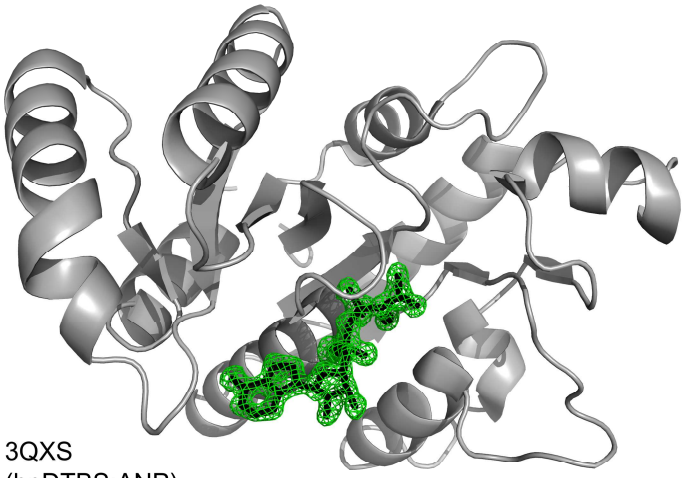

3QXS
(hpDTBS:ANP)

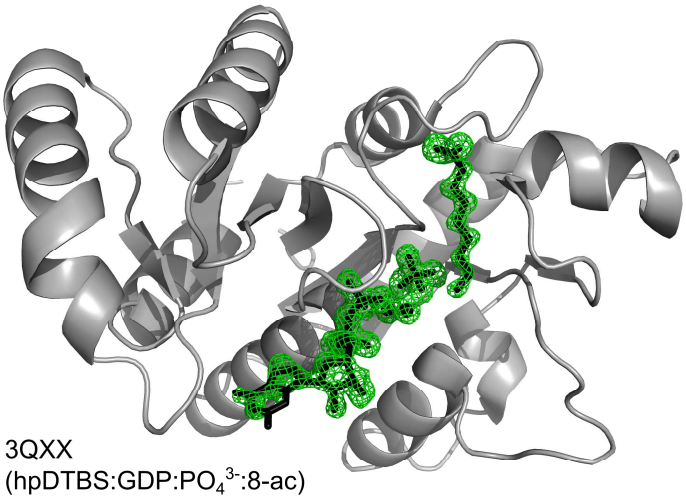

3QXX
(hpDTBS:GDP:PO_4^{3-}:8-ac)

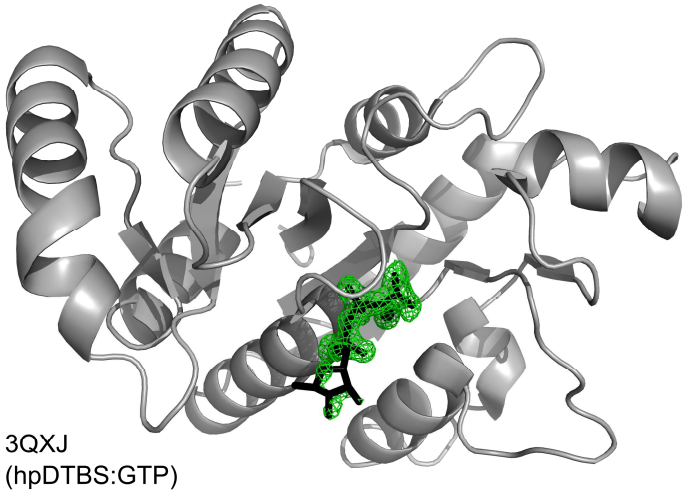

3QXJ
(hpDTBS:GTP)

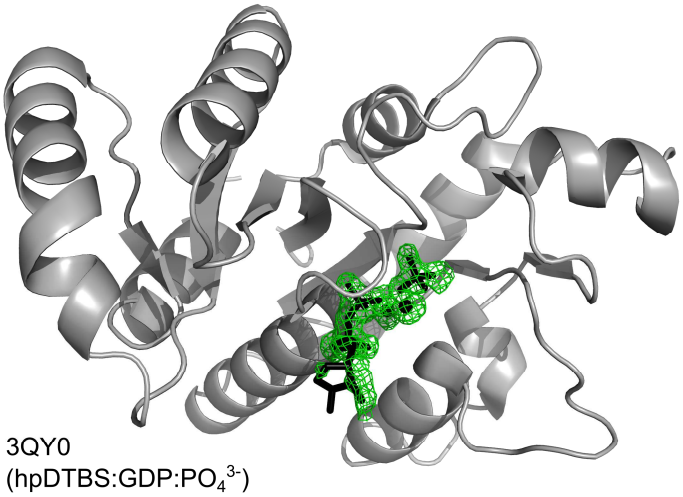

3QY0
(hpDTBS:GDP:PO_4^{3-})

Table S1

Species origin of sequences presented in Figure 6.

NCBI accession number	**Species origin**
YP_003783376.1	*Corynebacterium pseudotuberculosis*
YP_001854100.1	*Kocuria rhizophila*
YP_004099580.1	*Intrasporangium calvum*
YP_001551476.1	*Prochlorococcus marinus*
YP_003058961.1	*Hirschia baltica*
EAY55894.1	*Leptospirillum rubarum*
NP_884044.1	*Bordetella parapertussis*
YP_001280059.1	*Psychrobacter* sp. PRwf-1
YP_003967679.1	*Ilyobacter polytropus*
ZP_01960803.1	*Bacteroides caccae*
ADI18128.1	uncultured *Verrucomicrobiales*

Supplementary Methods

Generating non-redundant set of DTBS proteins

Since DTBS has been previously shown [1, 2] to be present in some fungi and plants as a fusion protein, sequences from *Eukaryota* were not included in further analysis. After the first iteration of PSI-BLAST, sequences with an E-value lower than 10^{-5} were collected for subsequent runs. For further PSI-BLAST iterations, only sequences with an E-value lower than 10^{-15} were retained. The search was performed with all other parameters set to default values using the NCBI BLAST server [3]. PSI-BLAST iterations were performed until no new sequences were found with an E-value lower than the assumed threshold. CLANS [4] was used to cluster the retrieved sequences according to the BLAST pairwise P-value scores. Sequences outside distinguishable clusters were inspected and removed when annotated as a ”putative” or ”hypothetical” protein, or when annotated as a different enzyme. Proteins annotated as putative that fell into well-defined clusters were retained in the analysis. The SKIPREDUNDANT program from the EMBOSS suite [5] was used to remove redundant sequences with 75% or greater sequence identity.

Crystallization and soaking

Native protein was crystallized by hanging-drop vapor diffusion using EasyXtal Tool (Qiagen) crystallization plates. Drops were formed by mixing 1 μL of mother liquor and 1 μL of either 27, 13.5 or 7 mg/mL of hpDTBS in 500 mM NaCl and 10 mM HEPES pH 7.5. Some of the crystals were soaked with, or crystallized in, various combinations of 10 mM each of ATP, guanosine-5’-triphosphate (GTP), adenosine-5’-diphosphate (ADP), guanosine-5’-diphosphate (GDP), adenosine 5’-(β,γ-imido) triphosphate (ANP), $MgCl_2$, and/or 8-aminocaprylic acid. Each 5 μL drop of soaking solution was formed by mixing 4 μL of mother liquor and 1 μL of additives before connection to the drop containing the crystal. Crystals were allowed to soak for at least 12 h before harvesting.

References

1. Hall, C. & Dietrich, F. S. (2007) The reacquisition of biotin prototrophy in Saccharomyces cerevisiae involved horizontal gene transfer, gene duplication and gene clustering, *Genetics.* **177**, 2293-2307.
2. Muralla, R., Chen, E., Sweeney, C., Gray, J. A., Dickerman, A., Nikolau, B. J. & Meinke, D. (2008) A bifunctional locus (BIO3-BIO1) required for biotin biosynthesis in Arabidopsis, *Plant Physiol.* **146**, 60-73.
3. Madden, T. L., Tatusov, R. L. & Zhang, J. H. (1996) Applications of network BLAST server, *Computer Methods for Macromolecular Sequence Analysis.* **266**, 131-141.
4. Frickey, T. & Lupas, A. (2004) CLANS: a Java application for visualizing protein families based on pairwise similarity, *Bioinformatics.* **20**, 3702-3704.
5. Rice, P., Longden, I. & Bleasby, A. (2000) EMBOSS: the European Molecular Biology Open Software Suite, *Trends Genet.* **16**, 276-7.